Synchronous Reluctance Machine modeling for accurate performances evaluation

Abstract - **The article gives an overview on different SynRM flux linkage and inductances estimation methods and assumptions in order to integrate nonlinear behavior of the machine, as well as the saturation and cross-saturation integration in the SynRM model. Analytical approach, Magnetic Equivalent Circuit and Finite Element analysis are used for magnetizing inductances and flux linkage computation, for two SynRM topologies.**

Keywords- synchronous reluctance machine, d- and q-axis inductances, linkage flux, cross-saturation, iron loss, look-up table based model, co-simulation.

Nomenclature

u_d, u_q – d and q-axis components of the stator voltage
torque
Ψ_d, Ψ_q – d and q-axis components of the stator linkage flux
torque
i_d, i_q- d and q-axis components of armature current
R_s – stator phase resistance
ω – rotor pulsation
T – electromagnetic torque
p-number of pole pairs
Ω – rotor mechanical speed
J – rotor inertia
B – damping coefficient
T_{load} – load torque
L_d, L_q- d and q-axis inductance
$L_{\sigma d}$, $L_{\sigma q}$- d and q-axis leakage inductance
L_{md}, L_{mq} - d and q-axis magnetizing inductance
k_C – Carter's factor
k_{sat} - saturation factor
δ_s – equivalent air-gap length
δ – d-axis airgap length
l_{by} – the length of the yth rotor flux barrier
ς – saliency ratio

I. Introduction

The potential of synchronous reluctance machine (SynRM) in automotive applications has been clearly demonstrated over the last years [1] [2] [3]. Its main advantages compare to induction machine are connected to the low-cost topology, "cold" rotor, high efficiency, good flux-weakening capabilities and high power density [4]. However, the low operating power factor, the high torque ripple content and the structural problems at high speeds asked for intensive work in order to optimize the rotor topology [5] [6] [7] [8] [9].

It is well known that both torque and power factor, as well as the dynamic response of SynRM drives are directly related to the d- and q-axis inductances. Moreover, the nonlinear behavior of the machine, including iron losses, saturation and cross-saturation, increases the complexity of its control and requests special attention in developing off- and on-line models for SynRM performances evaluation.

The present paper gives an overview on the influence of the machine parameters computation on the evaluation of SynRM drives performances. Two topologies will be analyzed, with the main data given in Table I.

TABLE 1. MAIN DATA OF THE SYNRMS UNDER STUDY

	SynRM_1	SynRM_2
Number of slots	24	27
Rotor radius	85.5 mm	
Shaft radius	22 mm	
Bridge thickness	1 mm	
Airgap length	1 mm	
Axial length	180 mm	

First analysis of the machine parameters was performed on SynRM_1 (with flux barrier optimized shapes) [10] [11], then, the analysis focused on SynRM_2, a topology resulted after a multi-objective optimization process, with improved electromagnetic performances and structural behavior [12].

II. SynRM model

The equations defining the behavior of SynRM in rotor dq-co-ordinates are as follows [13]:

$$u_d = R_s i_d + \frac{\partial \Psi_d}{\partial t} - \omega \Psi_q \tag{1}$$

$$u_q = R_s i_q + \frac{\partial \Psi_q}{\partial t} + \omega \Psi_d \tag{2}$$

$$T = \frac{3}{2} p\left(\Psi_d i_q - \Psi_q i_d\right) \tag{3}$$

$$T = J\frac{d\Omega}{dt} + B\Omega + T_{load} \tag{4}$$

The complexity of the control and the accuracy of

The results presented in this paper are part of a project that has received funding from the European Union's Horizon 2020 research and innovation programme under grant agreement No XXXXXX.

performances evaluation depend on the computation method for d- and q- axis linkage fluxes. Several approaches are described and applied for the machines under study.

Fig. 1 presents the cross-section of the two SynRM under study.

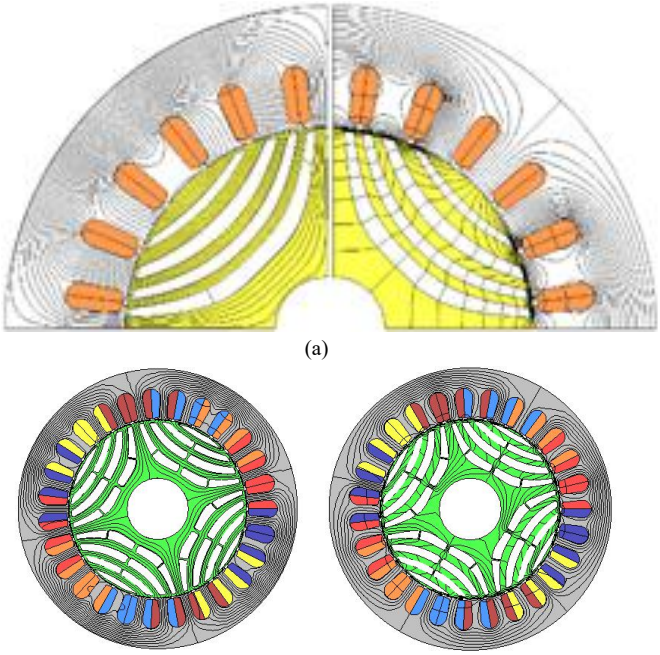

(a)

(b)

Fig. 1 Cross-section and d- and q-axis flux lines ((left and right side of the figure) of SynRM_1(a) and SynRM_2 (b)

III. Decoupled linear and non-linear SynRM models

In a first approximation, the d- and q-axis flux linkages can be written as:

$$\Psi_d = L_d i_d$$
$$\Psi_q = L_q i_q \tag{5}$$

and Eq (1) and (2) :

$$u_d = R_s i_d + L_d \frac{\partial i_d}{\partial t} - \omega L_q i_q \tag{6}$$

$$u_q = R_s i_q + L_q \frac{\partial i_q}{\partial t} + \omega L_d i_d \tag{7}$$

and the electromagnetic torque results as:

$$T = \frac{3}{2} p\left(L_d - L_q\right) i_q i_d \tag{8}$$

Moreover, the maximum power factor is given by:

$$\cos\varphi_{\max} = \frac{\frac{L_d}{L_q} - 1}{\frac{L_d}{L_q} + 1} = \frac{\varsigma - 1}{\varsigma + 1} \tag{9}$$

Thus, the machine is completely defined and its performances can be evaluated once the L_d and L_q values are available. There are different methods, theoretical and experimental to compute direct and quadrature inductances, taking or not taking into account the nonlinear behavior of the machine and the iron losses, depending on how accurate the behavior of the machine has to be described.

A. *Analytical – based computation of direct and quadrature inductances*

The simplest SynRM inductances computation method is based on the fundamental magnetizing and leakage inductances calculation; thus L_d and L_q are given as:

$$L_d = L_{\sigma s} + L_{md}$$
$$L_d = L_{\sigma s} + L_{md} \tag{10}$$

with L_{md} given by [teza TMP]:

$$L_{md} = \frac{m}{\pi} \frac{\mu_0}{\delta_{sd}} DL \left(\frac{w_1}{p}\right)^2 k_{w1}^2 \tag{11}$$

where:

$$\delta_{sd} = k_C k_{sat} \delta \tag{12}$$

The analytical computation of quadrature axis inductance L_q is difficult due to the different saturation degrees of the rotor core and to the complex path of q-axis flux. A rough estimation of L_q can however be done by considering the q-axis air-gap length as to include the sum thickness of the flux barriers, but without taking into account the effects of the rotor saturated iron ribs and webs:

$$\delta_{sq} = k_C k_{sat} \delta + \sum_y l_{by} \tag{13}$$

Analytical calculation of d- and q- axis leakage inductances is rather difficult as the geometry of the leakage flux lines is complicated. As their values are very small compared to the magnetizing direct and quadrature inductances, they can be ignored.

The application of the presented method is limited since it only gives constant inductances of the machine. In order to include saturation of the iron core or rotor position impact on the inductances, other methods should be used.

B. *Direct and quadrature inductances computation by taking into account the nonlinearity of the magnetic circuit*

For a nonlinear decoupled SynRM, the direct axis inductance depends only on i_d current and the quadrature axis inductance depends only on i_q current. Based on such an assumption, the computation of L_d and L_q requires more elaborated methods and tools.

For analytical calculations, using lumped circuit models (Magnetic equivalent circuits – MECs), due to the flux barriers in the rotor changing the reluctance of the magnetic circuit and hence modifying the path for magnetic flux that links the stator and rotor, difficulties in modeling of SynRM are generated. As the machine behaves differently when the magnetomotive force is applied in d or q axis, respectively, two separate MEC models of the machine were developed [].

The analysis of MEC models based on reluctance network(s) seems to be convenient and quite easy method for the evaluation of the SynRM performances. Different rotor topologies of SynRMs require different mathematical

approaches since the shapes of flux barriers are based on various mathematical curves. Specific approach was developed for the machine with Zhukovski flux barriers [] defined by implicit functions which make computation more difficult.

A more accurate, but higher time and resources consuming computation of L_d and L_q can be done by using Finite Element (FE) based analysis. The model of the machine is implemented in a FE-based software package and the magnetostatic analysis is done at different rotor positions and for different i_d and i_q currents.

Direct and quadrature inductances L_d and L_q can be then computed as derivative of flux linkage with respect to current i_d and i_q:

$$L_d = \frac{d\Psi_d}{di_d}\Big|_{i_q=cst} \approx \frac{\Delta\Psi_d}{\Delta i_d}\Big|_{i_q=cst} \tag{13}$$

$$L_q = \frac{d\Psi_q}{di_q}\Big|_{i_d=cst} \approx \frac{\Delta\Psi_q}{\Delta i_q}\Big|_{i_d=cst} \tag{14}$$

For a Zhukovski flux barriers SynRM [] with the main data given in Table 1 both MEC and FE analysis was performed and the variation of direct and quadrature inductances with i_d and i_q currents is presented in Figure X.

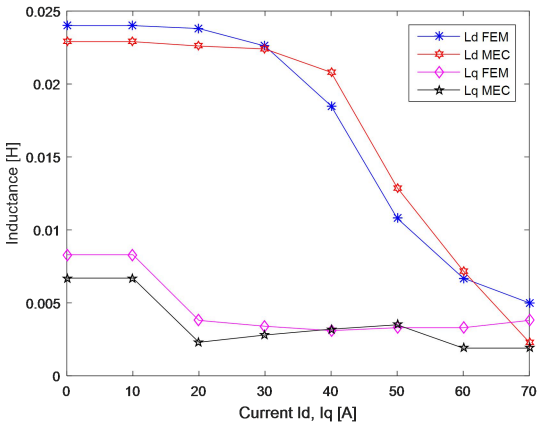

Fig. 2 Direct and quadrature inductances

As it can be noticed in Fig. 2, the results of MEC and FE models are similar. Even if this proves that MEC model provides acceptable accuracy in SynRM inductances calculation, the difference between the results demonstrates that saturation and cross-saturation represents a phenomenon with an important impact on the machine performances evaluation.

IV. Coupled non-linear SynRM models

If the cross-saturation phenomenon is taken into account, the d- and q-axis flux linkages can be written as:

$$\begin{aligned} \Psi_d &= L_d i_d + L_{qd} i_q \\ \Psi_q &= L_q i_q + L_{dq} i_d \end{aligned} \tag{15}$$

with L_d, L_q, L_{qd} and L_{dq} dependent on both i_d and i_q. Thus Eq. (1) and (2) become:

$$u_d = R_s i_d + L_d \frac{\partial i_d}{\partial t} - \omega L_q i_q + L_{qd} \frac{\partial i_q}{\partial t} \tag{16}$$

$$u_q = R_s i_q + L_q \frac{\partial i_q}{\partial t} + \omega L_d i_d + L_{dq} \frac{\partial i_d}{\partial t} \tag{17}$$

In order to calculate the inductances of the machine 2D and 3D FE analysis was performed. Moreover, the influence of skewing the rotor on the machine parameters will be estimated. The machine under study corresponds to SynRM_2.

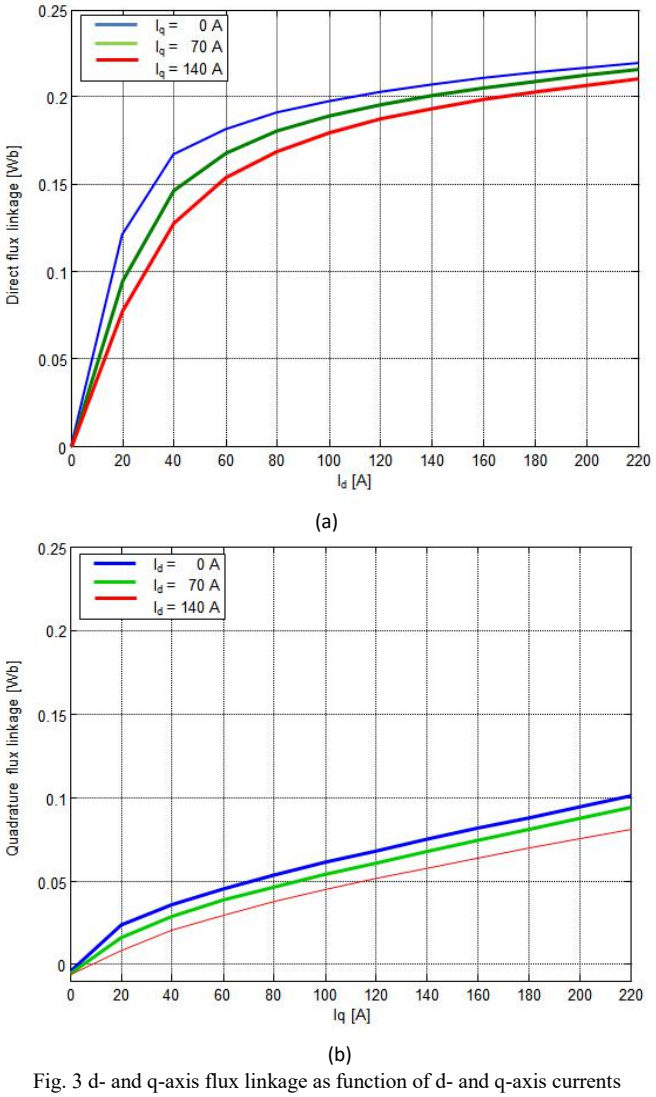

Fig. 3 d- and q-axis flux linkage as function of d- and q-axis currents

As it can be noticed in Fig. 3a d axis flux linkage rises very quickly with i_d current and eventually saturates. This is because the flux path in d axis of the rotor mostly consists of iron flux paths. The magnetic field in d axis almost completely avoids air flux barriers in the rotor. The presence of i_q component generates a decrease of the flux linkage in d axis.

Fig. 3b presents q axis flux linkage which increases almost linearly with i_q current. This is caused by the presence of flux barriers in the rotor which are penetrated by magnetic field. The presence of the air in the path of magnetic flux significantly increases the reluctance of q axis magnetic circuit. In this case, when i_d component of phase current is present, the q axis flux linkage decreases similarly as in case of d axis flux linkage.

Fig.4a shows the impact of cross saturation on d axis flux linkage. If there was no cross saturation, the flux linkage in d axis would depend on d axis current only and it would remain constant regardless the variations of q axis current. However, increasing q axis current causes the flux linkage in d axis to drop. This phenomenon is stronger for low d axis current and lowers when the current in d axis increases. Similarly q axis flux drops when the current in d axis grows. Variations of q axis flux linkage are greater than those of d axis flux. This situation is presented in Fig. 4b.

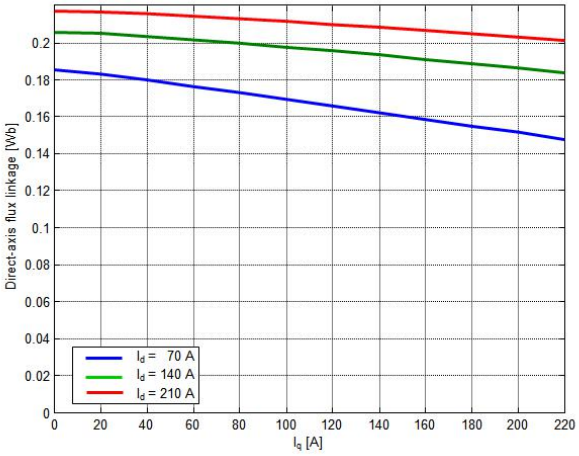

(a)

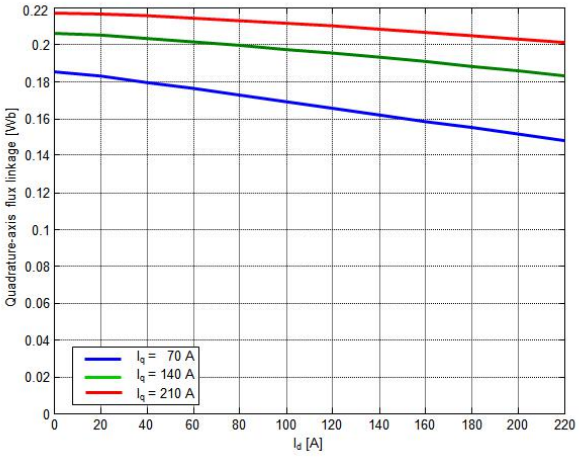

(b)

Fig. 4 d- and q-axis flux linkage as function of q- and d-axis currents respectively

If there was no cross saturation, the flux linkage in d axis would depend on d axis current only and it would remain constant regardless the variations of q axis current. However, increasing q axis current causes the flux linkage in d axis to drop. This phenomenon is stronger for low d axis current and lowers when the current in d axis increases. Similarly q axis flux drops when the current in d axis grows. Variations of q axis flux linkage are greater than those of d axis flux.

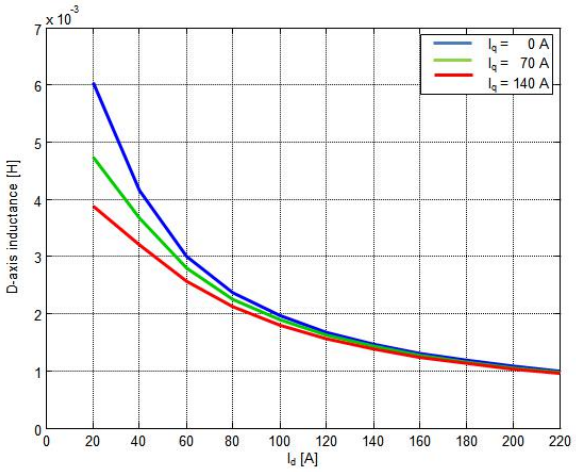

(a)

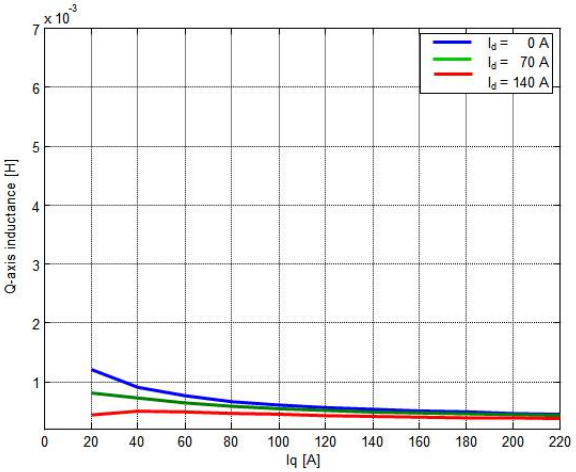

(b)

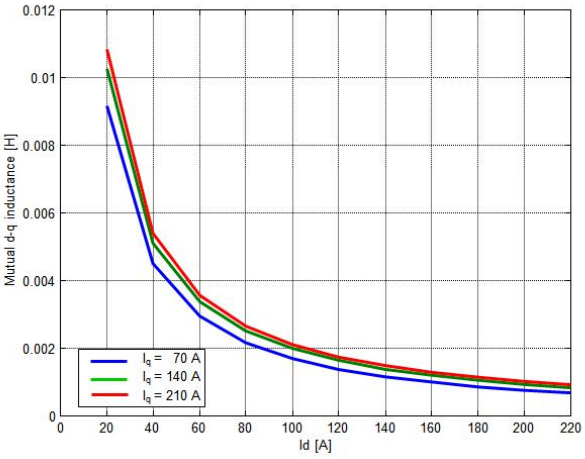

(c)

Fig. 5 Direct, quadrature and mutual inductances as function of q- and d-axis current

Presence of cross saturation means that inductances in d and q axes are also functions of two currents and there is a mutual inductance between d and q axis equivalent circuits.

$$L_d(i_d,i_q)=\frac{\partial\Psi_d(i_d,i_q)}{\partial i_d}|_{i_q=cst} \quad (18)$$

$$L_q(i_d,i_q)=\frac{\partial\Psi_q(i_d,i_q)}{\partial i_q}|_{i_d=cst} \quad (19)$$

$$L_{dq}(i_d,i_q)=\frac{\partial\Psi_d(i_d,i_q)}{\partial i_q}|_{i_d=cst} \quad (20)$$

$$L_{qd}(i_d,i_q)=\frac{\partial\Psi_q(i_d,i_q)}{\partial i_d}|_{i_d=cst} \quad (21)$$

with $L_{dq}=L_{qd}$. Machine's d and q inductances are shown below. Values of inductances decrease as the currents grow. This is due to saturation of the magnetic circuit of the motor. Inductances of the machine in d and q axes are presented in Fig. 5 as functions of the two currents, i_d and i_q.

Rotor skew has a significant impact on machine's flux linkage. In case of d axis MMF skewing the rotor results in lower flux linkage. The orthogonal axes (d and q) of a skewed rotor cannot be aligned with orthogonal axes of the stator. Rotor in d axis provides a magnetic path of the smallest reluctance.

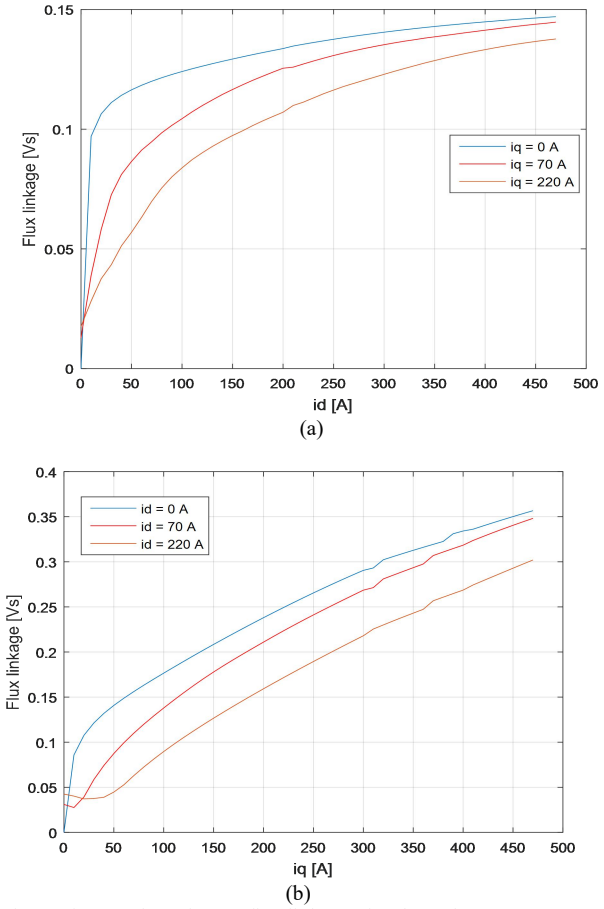

Fig. 6 Direct and quadrature flux linkages for skewed rotor SynRM_2

Flux linkage in d axis achieves the maximum value at a given current hence any deviation from this position increases the reluctance of d axis magnetic circuit. Exact opposite situation occurs in for q axis MMF. Since the magnetic circuit in q axis has the highest magnetic reluctance, any deviation from q axis results in increased magnetic flux flowing between the stator and the rotor. For that reason, the flux linkage in q axis is sometimes higher than flux linkage in d axis for machine with skewed rotor. However, the cross saturation is also higher in machine with skewed rotor especially for q axis flux linkage. Fig. 6 presents the d- and q-axis flux linkage vs the d- and q-axis current, respectively, taking into account also the cross-saturation.

V. Conclusions

The present paper gives an overview on different SynRM flux linkage and inductances estimation methods and assumptions. The nonlinear behavior of the machine, as well as the saturation and cross-saturation integration in the SynRM model will contribute to increasing the accuracy of the performances evaluation at drive level.

VI. References

[1] Reza Rajabi Moghaddam, "Synchronous reluctance machine (SynRM) design", Master Thesis, Stockholm 2007.

[2] Reza Rajabi Moghaddam, Freddy Gyllensten, "Novel high-performance SynRM design method: An easy approach for a complicated rotor topology" IEEE Transactions on Industrial Electronics, Vol: 61, No: 9, September 2014, pp: 5058-5065, ISSN: 0278-0046.

[3] S. Tahi, R. Ibtiouen, M. Bounekhla: "Design Optimization of Two Synchronous Reluctance Machine Structures with Maximized Torque and Power Factor", Progress in Electromagnetics Research, Vol. 35, 2011.

[4] Reza - Rajabi Moghaddam, "Synchronous reluctance machine (SynRM) in variable speed drives (VSD) applications", Doctoral Thesis, Stockholm, Sweden, 2011

[5] K. T. Chau, Senior Member, IEEE, Qiang Sun, Ying Fan, "Torque ripple minimization of doubly salient permanent-magnet motors", IEEE Transactions on Energy Conversion, Vol. 20, No. 2, June 2005

[6] S. Tahi, R. Ibtiouen, M. Bounekhla: "Design Optimization of Two Synchronous Reluctance Machine Structures with Maximized Torque and Power Factor", Progress in Electromagnetics Research, Vol. 35, 2011.

[7] Jere Kohelmainen: "Synchronous Reluctance Motor With Form Blocked Rotor", IEEE Transactions on Energy Conversion, Vol. 25, No. 2, June, 2010.

[8] Xola B. Bomela, Maarten J. Kamper: "Effect of Stator Chording and Rotor Skewing on Performance of Reluctance Synchronous Machine", IEEE Transactions on Industry Applications", IEEE Transactions on Industry Applications, Vol. 38, No. 1, January/February, 2002.

[9] Erich Schmidt, Wolfgang Brandl: "Comparative Finite Element Analysis of Synchronous Reluctance Machines with Internal Rotor Flux Barriers", IEEE, 2001.

[10] Arkadiusz Dziechciarz, Claudia Martis: "New Shape of Rotor Flux Barriers in Synchronous Reluctance Machines Based on Zhukovski Curves", The 9th International Symposium on ADVANCED TOPICS IN ELECTRICAL ENGINEERING (ATEE), 7-9 May 2015 Bucharest, DOI: 10.1109/ATEE.2015.7133768.

[11] Arkadiusz Dziechciarz ; Claudia Martis: „Simplified model of synchronous reluctance machine with optimized flux barriers", Electrical Engineering, Volume 99 / 2017, ISSN 0948-7921, Publisher Springer Berlin Heidelberg.

[12] Arkadiusz Dziechciarz ; Claudiu Oprea ; Claudia Martis, Multi-physics design of synchronous reluctance machine for high speed applications, IECON 2016 - 42nd Annual Conference of the IEEE

Industrial Electronics Society, ISBN: 978-1-5090-3474-1, 10.1109/IECON.2016.7793986

[13] Mircea Ruba; Florin Jurca ; Claudia Martis Analysis of synchronous reluctance machine for light electric vehicle applications, 2016 International Symposium on Power Electronics, Electrical Drives, Automation and Motion (SPEEDAM), ISBN: 978-1-5090-2067-6, 10.1109/SPEEDAM.2016.7525841 22-24 June 2016

[14] Arkadiusz Dziechciarz ; Claudia Martis, Magnetic equivalent circuit of synchronous reluctance machine, ELEKTRO 2016, ISBN: 978-1-4673-8698-2, 10.1109/ELEKTRO.2016.7512126